PTP1B inhibition ameliorates inflammatory injury and dysfunction in ox-LDL-induced HUVECs by activating the AMPK/SIRT1 signaling pathway via negative regulation of KLF2

YUNFENG ZHANG, QIANG GUAN and ZHENFENG WANG

Department of Vascular Surgery, Shanxi Provincial People's Hospital, Taiyuan, Shanxi 030012, P.R. China

Abstract. Atherosclerosis is a key pathogenic factor of cardiovascular diseases. However, the role of protein tyrosine phosphatase 1B (PTP1B) in oxidized low-density lipoprotein (ox-LDL)-treated vascular endothelial cells remains unclear. The aim of the present study was to explore the possible physiological roles and mechanism of PTP1B in atherosclerosis using HUVECs as an *in vitro* model. PTP1B expression was assessed by reverse transcription-quantitative PCR. Cell viability was measured using the Cell Counting Kit-8 and lactate dehydrogenase activity assays. Levels of inflammatory factors, including IL-1β, IL-6 and TNF-α, and oxidative stress factors, including malondialdehyde, superoxide dismutase and glutathione peroxidase, were assessed using ELISA and commercially available kits, respectively. Furthermore, TUNEL assay and western blotting were performed to assess the extent of apoptosis-related factors, including Bcl-2, Bax, Cleaved caspase-3 and Caspase-3. Tube formation assay was used to assess tubule formation ability and western blotting was to analyze VEGFA protein level. Binding sites for the transcription factor Kruppel-like factor 2 (KLF2) on the PTP1B promoter were predicted using the JASPAR database and verified using luciferase reporter assays and chromatin immunoprecipitation. The protein levels of phosphorylated 5'AMP-activated protein kinase (p-AMPK), AMPK and SIRT1 were measured using western blotting. The results demonstrated that the PTP1B mRNA and protein expression levels were significantly upregulated in oxidized low-density lipoprotein (ox-LDL)-induced HUVECs. In addition, ox-LDL-induced HUVECs transfected with short hairpin RNA against PTP1B exhibited a significant increase in cell viability, reduced inflammatory factor levels, apoptosis and oxidative stress, as well as increased tubule formation ability. KLF2 was found to negatively regulate the transcriptional activity of PTP1B. KLF2 knockdown reversed the protective effects of PTP1B knockdown on ox-LDL-induced HUVECs. KLF2 knockdown also abolished PTP1B knockdown-triggered AMPK/SIRT1 signaling pathway activation in ox-LDL-induced HUVECs. To conclude, the results of the present study suggested that PTP1B knockdown can prevent ox-LDL-induced inflammatory injury and dysfunction in HUVECs, which is regulated at least in part by the AMPK/SIRT1 signaling pathway through KLF2.

Introduction

Endothelial cells (ECs) serve to maintain vascular integrity and homeostasis by sensing and responding to pathological and physiological stimuli (1-4). During the onset of vascular disease, major phenotypical alterations occur in the ECs, resulting in increased vascular permeability, release of large quantities of inflammatory cytokines (IL-8, IL-6 and IL-1β) and leukocyte adhesion (5-7). These pathological changes in the blood vessel wall structure and function in turn increases the risk of atherosclerosis (8-10). It has previously been reported that EC inflammation and apoptosis serve key roles in the initiation and development of atherosclerosis, hypertension, diabetes and other cardiovascular diseases (11). Furthermore, endothelial dysfunction is regarded to be one of the first stages in the pathophysiology of atherosclerosis (12). Loss of morphological and functional integrity in vascular ECs has been reported to be attributed to inflammation and apoptosis (13). Therefore, therapeutic strategies targeting inflammation, apoptosis and vascular EC dysfunction may be important for the treatment of atherosclerosis.

Protein tyrosine phosphatase 1B (PTP1B) is a non-transmembrane protein tyrosine phosphatase that has been documented to be a negative regulator in diabetes and obesity signaling (14-16). In addition, it has reported roles in the malignant transformation of various cancers, including pancreatic cancer and resistance in cancer treatments, such

Correspondence to: Dr Yunfeng Zhang, Department of Vascular Surgery, Shanxi Provincial People's Hospital, 29 Shuangta East Street, Taiyuan, Shanxi 030012, P.R. China
E-mail: zhangyunfeng82@126.com

Abbreviations: PTP1B, protein tyrosine phosphatase 1B; ox-LDL, oxidized low-density lipoprotein; KLF2, Kruppel-like factor 2; ECs, endothelial cells; CCK-8, Cell Counting Kit-8; LDH, lactate dehydrogenase; RT-qPCR, reverse transcription-quantitative PCR; MDA, malondialdehyde; SOD, superoxide dismutase; GSH-Px, glutathione peroxidase; ChIP, chromatin immunoprecipitation

Key words: atherosclerosis, PTP1B, KLF2, ox-LDL, inflammation, transcription factor

as dendritic cell-based cancer immunotherapy (14-16). Accumulating evidence indicates that PTP1B is also involved in atherosclerosis (17). Thompson *et al* (18) previously reported that PTP1B inhibitors can prevent and reverse atherosclerotic plaque formation in low-density lipoprotein (LDL) receptor$^{-/-}$ mice with atherosclerosis, thereby reducing the risk of cardiovascular disease. Improved glucose homeostasis, reduced circulating lipids and atherosclerotic plaque lesions, have also been observed in myeloid-PTP1B-knockout mice (apolipoprotein E$^{-/-}$/lysozyme M-PTP1B) with atherosclerosis (19). In addition, endothelial PTP1B has been reported to serve as the main regulator of EC proliferation in cardiovascular disease (20). By contrast, PTP1B depletion was found to induce endothelium-dependent vasorelaxation in microvessels in animal models of heart failure and diabetes (21,22). However, to the best of our knowledge, the potential effects of PTP1B on the inflammation, apoptosis and dysfunction of oxidized (ox)-LDL-induced vascular ECs and associated mechanisms remain unreported.

Therefore, the present study aimed to investigate the possible role of PTP1B in ox-LDL-treated HUVECs. The study reported the efficacy of PTP1B on the proliferation, inflammation, apoptosis, oxidative stress, tubule formation, Kruppel-like factor 2 (KLF2) and 5'AMP-activated protein kinase (AMPK)/sirtuin 1 (SIRT1) signaling pathway in ox-LDL-induced HUVECs through functional experiments and mechanism assays.

Materials and methods

Cell culture. Immortalized HUVECs were purchased from Shanghai EK-Bioscience Biotechnology Co., Ltd. (cat. no. CC-Y1285). Cells were cultured in DMEM (Gibco; Thermo Fisher Scientific, Inc.) supplemented with 10% FBS (Hyclone; Cytiva) and 1% penicillin/streptomycin in a humidified atmosphere containing 5% CO_2 at 37˚C. To establish an *in vitro* atherosclerosis model, HUVECs were treated with 100 μg/ml ox-LDL (Guangzhou Yiyuan Biological Technology Co., Ltd.) for 24 h at 37˚C. Untreated cells were regarded as the control group.

Transfection. The short hairpin (sh)RNA targeting PTP1B (sh-PTP1B#1/2), KLF2 (sh-KLF2#1/2) and the corresponding sh-negative control (NC; sh-NC) were synthesized and inserted into the pRNA-U6.1 plasmid (GenScript) by GeneCopoeia, Inc. The sequences of shRNAs were as follows: sh-PTP1B#1, 5'-GCTACAGGTTCCTGTTCAA-3'; sh-PTP1B#2, 5'-GGT TCCTGTTCAACAGCAA-3'; sh-KLF2#1, 5'-GCACCGACG ACGACCTCAA-3'; sh-KLF2#2, 5'-GAGTGGTAGCTTTCT ACAA-3'; sh-NC, 5'-CCGGCAACAAGATGAAGAGCACCA ACTC-3'.

A pcDNA3.1 overexpression vector (GenScript) encoding the full-length KLF2 (Ov-KLF2) and the corresponding NC (Ov-NC) were produced by Shanghai GenePharma Co., Ltd. In total, 100 nM recombinant vectors were transfected into HUVECs for 48 h using Lipofectamine® 2000 (Invitrogen; Thermo Fisher Scientific, Inc.) according to the manufacturer's protocol at 37˚C. The transfected HUVECs were then collected for subsequent experiments.

Cell Counting Kit (CCK)-8 assay. HUVECs ($4x10^4$ cells/well) seeded into a 96-well plate were transfected with sh-PTP1B in the presence or absence of sh-KLF2 before treatment with ox-LDL (100 μg/ml) for 24 h at 37C (23-25). Subsequently, 10 μl CCK-8 solution (Beyotime Institute of Biotechnology) was added to each well and the plates were incubated for 2 h at 37˚C. The optical density values were analyzed using a Thermo Multiskan FC microplate reader (Thermo Fisher Scientific, Inc.) at 450 nm.

Lactate dehydrogenase (LDH) activity assay. HUVECs plated at a density $1x10^4$ cells/well in 96-well plates were transfected with sh-PTP1B in the presence or absence of sh-KLF2 and underwent ox-LDL treatment (100 μg/ml) for 24 h at 37˚C. Cells were subsequently harvested from the culture plate and the LDH activity levels were detected by LDH activity kit (cat. no. A020; Nanjing Jiancheng Bioengineering Institute) at 450 nm using a microplate reader (Thermo Fisher Scientific, Inc.).

ELISA. Briefly, HUVECs were seeded into 96-well plates ($5x10^3$ cells/well). Following the aforementioned treatment, cell supernatant was collected after centrifugation at 2,000 x g for 5 min at 4˚C. IL-6 (cat. no. ab178013), IL-1β (cat. no. ab214025) and TNF-α (cat. no. ab181421) levels in the culture supernatant were determined using ELISA kits from Abcam according to the manufacturer's protocols. The absorbance was determined at 450 nm using an xMark microplate absorbance spectrophotometer (Bio-Rad Laboratories, Inc.).

Reverse transcription-quantitative PCR (RT-qPCR). Total RNA was extracted from HUVECs using the TRIzol® reagent (Invitrogen; Thermo Fisher Scientific, Inc.). Subsequently, the quality and purity of the extracted RNA were detected using a NanoDrop® 3000 spectrophotometer (Thermo Fisher Scientific, Inc.). Total RNA was reverse-transcribed into complementary DNA using the PrimeScript™ RT Master Mix (Takara Bio, Inc.) according to the manufacturer's instructions. qPCR was performed using the SYBR Premix Ex Taq™ II kit (Takara Bio, Inc.). The following thermocycling conditions were used: 95˚C for 7 min; 45 cycles of denaturation at 95˚C for 10 sec, annealing at 60˚C for 15 sec and extension at 72˚C for 30 sec; final extension at 60˚C for 1 min followed by cooling at 40˚C for 5 min. The following primers were used for qPCR: PTP1B forward (F), 5'-GCGGCCATTTACCAGTTG AC-3' and reverse (R), 5'-ATGACGACACCCCTGCTTTT-3'; KLF2 F, 5'-TGGGCATTTTTGGGCTACCT-3' and R, 5'-GTC AGTGGGACCAGCACTTT-3'; and GAPDH F, 5'-GGGAAA CTGTGGCGTGAT-3' and R, 5'-GAGTGGGTGTCGCTG TTGA-3'. Relative mRNA expression levels were normalized to GAPDH using the $2^{-\Delta\Delta Cq}$ method (26).

TUNEL assay. Cell apoptosis was detected using an *In Situ* Cell Death Detection Kit (cat. no. 11684817910; Roche Diagnostics GmbH). Cells were fixed with 4% paraformaldehyde at room temperature away from light for 30 min and then incubated with proteinase K for 15 min in 37˚C. Subsequently, cells were placed in 3% H_2O_2 for 15 min at room temperature to inhibit endogenous peroxide. HUVECs were then stained with the TUNEL detection kit at 37˚C for 60 min and co-labeled

with the DAPI working solution (1 μg/ml) for 10 min at 37°C according to the manufacturer's protocols. Labeled HUVECs were washed with PBS buffer. Next, cells on slips were mounted using DAPI-containing mounting medium (Vector Laboratories, Inc.) and visualized using a fluorescence microscope (Nikon Eclipse 80i; Nikon Corporation), and >10 fields per section for each sample were examined. The TUNEL positive cell rate (%) was calculated using the software of Developer XD 1.2 (Definiens AG) according to the following formula: (Number of positive cells/total number of cells) x100.

Malondialdehyde (MDA), superoxide dismutase (SOD) and glutathione peroxidase (GSH-Px) assays. HUVECs were seeded into 96-well plates (5x10^3 cells/well). After transfection of sh-PTP1B in the presence or absence of sh-KLF2 and ox-LDL treatment (100 μg/ml) for 24 h at 37°C, oxidative stress levels were quantified by detecting the levels of MDA (cat. no. A003-4-1) and the activity of SOD (cat. no. A001-3-2) and GSH-Px (cat. no. A005-1-2) in the media using the corresponding commercial kits (Nanjing Jiancheng Bioengineering Institute) according to the manufacturer's protocols. Absorbance at 532 nm was measured using a microplate reader (BioTek Instruments, Inc.).

Endothelial tube formation assay. HUVECs were seeded at a density of 5x10^3 cells/well into 96-well plates pre-coated with 50 μl/well Matrigel (Corning, Inc.) at 37°C for 2 h. HUVECs were seeded into 96-well plates and transfected with sh-PTP1B in the presence or absence of sh-KLF2 and underwent ox-LDL treatment (100 μg/ml). Following incubation for 24 h at 37°C, tubules characterized by the capillary-like structures were imaged using a light microscope in five randomly selected fields (magnification, x40).

Dual-luciferase reporter assay. Briefly, the potential interaction between KLF2 and the PTP1B promoter were predicted using data from the 9th release (2022) of JASPAR database (http://jaspar.genereg.net). The wild-type and mutant PTP1B promoter fragments, including predicted KLF2 sites, were amplified and cloned downstream of the luciferase reporter gene in the firefly luciferase reporter pGL3 vector (Promega Corporation). HUVECs were transfected with 2.5 μg Ov-KLF2 or 2.5 μg Ov-NC plasmids, with 100 ng of luciferase reporter plasmids driven by wild-type or mutant PTP1B promoter, using Lipofectamine 2000 at 37°C for 48 h before luciferase activity was detected using the Dual-Luciferase Reporter Assay Kit (Promega Corporation). Firefly luciferase activity was normalized to *Renilla* luciferase activity.

Chromatin immunoprecipitation (ChIP). ChIP experiments were performed using the ChIP-IT kit (cat. no. 53008; Active Motif, Inc.) according to the manufacturer's instructions as previously described (27). Briefly, HUVECs were cross-linked with 1% formaldehyde at 37°C for 10 min. The cell lysates were sonicated using a 10 sec on and 10 sec off mode for 12 cycles on ice. Following quenching with 2.5 M glycine for 5 min at room temperature, the supernatant was collected, added to 60 μl Protein A Agarose beads (cat. no. 9863; Cell Signaling Technology, Inc.) and mixed for 1 h after centrifugation. DNA was immunoprecipitated from the 100 μl cell lysates using

2 μg KLF2 antibody (cat. no. MBS9211982; MyBioSource) for a 2-h incubation at 4°C. The beads were washed using a magnetic separation rack and the bound chromatin was eluted in ChIP Elution Buffer with Proteinase K mixer. PCR amplification of the PTP1B binding site was then performed using the precipitated DNA by means of SYBR Premix Ex Taq™ II kit (cat. no. RR420A; Takara Bio, Inc.). The following thermocycling conditions were used: 95°C for 7 min, followed by 45 cycles of denaturation at 95°C for 10 sec, annealing at 60°C for 15 sec and extension at 72°C for 30 sec, with a final extension at 60°C for 1 min followed by cooling at 40°C for 5 min. Next, the immunoprecipitated DNA was purified using a ChIP DNA purification kit (cat. no. D0033; Beyotime Institute of Biotechnology). Nonspecific antibody against IgG (2 μg; 1:40; cat. no. sc-2025; Santa Cruz Biotechnology, Inc.) served as a negative control.

Western blotting. Total protein was isolated from HUVECs using RIPA buffer (Beyotime Institute of Biotechnology). The protein concentration was determined using a BCA protein assay kit (Beyotime Institute of Biotechnology). A total of 30 μg protein was separated using SDS-PAGE on a 10% gel (Bio-Rad Laboratories, Inc.) and transferred onto PVDF membranes (MilliporeSigma). After being blocked with 5% non-fat milk for 1 h at room temperature, the membranes were incubated with primary antibodies targeting PTP1B (1:1,000; cat. no. ab244207; Abcam), Bcl-2 (1:1,000; cat. no. ab196495; Abcam), Bax (1:1,000; cat. no. ab32503; Abcam), cleaved caspase-3 (1:500; cat. no. ab32042; Abcam), caspase-3 (1:5,000; cat. no. ab32351; Abcam), vascular endothelial growth factor A (VEGFA; 1:1,000; cat. no. ab155944; Abcam), KLF2 (1:1,000; cat. no. ab194486; Abcam), phosphorylated (p)-AMPK (1:1,000; cat. no. ab92701; Abcam), AMPK (1:1,000; cat. no. ab32047; Abcam), SIRT1 (1:1,000; cat. no. ab110304; Abcam) and GAPDH (1:1,000; cat. no. ab8245; Abcam) overnight at 4°C. Following the primary incubation, the membranes were incubated with the HRP-conjugated goat anti-rabbit or mouse secondary antibodies (cat. nos. sc-2004 or sc-2005; 1:5,000; Santa Cruz Biotechnology, Inc.) at room temperature for 1 h. The bands were visualized using the Pierce™ Enhanced Chemiluminescence (ECL) Western Blotting Substrate Kit (Invitrogen; Thermo Fisher Scientific, Inc.) and quantified by densitometry (Quantity One 4.5.0 software; Bio-Rad Laboratories, Inc.). All data were normalized to that of GAPDH.

Statistical analysis. All statistical analysis was performed using GraphPad Prism software (version 5.01; GraphPad Software, Inc.). All data are presented as the mean ± SD from at least three independent experiments. Statistical comparisons between two groups were performed using unpaired Student's t-test, whereas comparisons among >2 groups was performed using one-way ANOVA followed by Bonferroni post hoc test. $P < 0.05$ was considered to indicate a statistically significant difference.

Results

PTP1B knockdown restores cell viability in ox-LDL-induced HUVECs. To investigate the role of PTP1B in atherosclerosis,
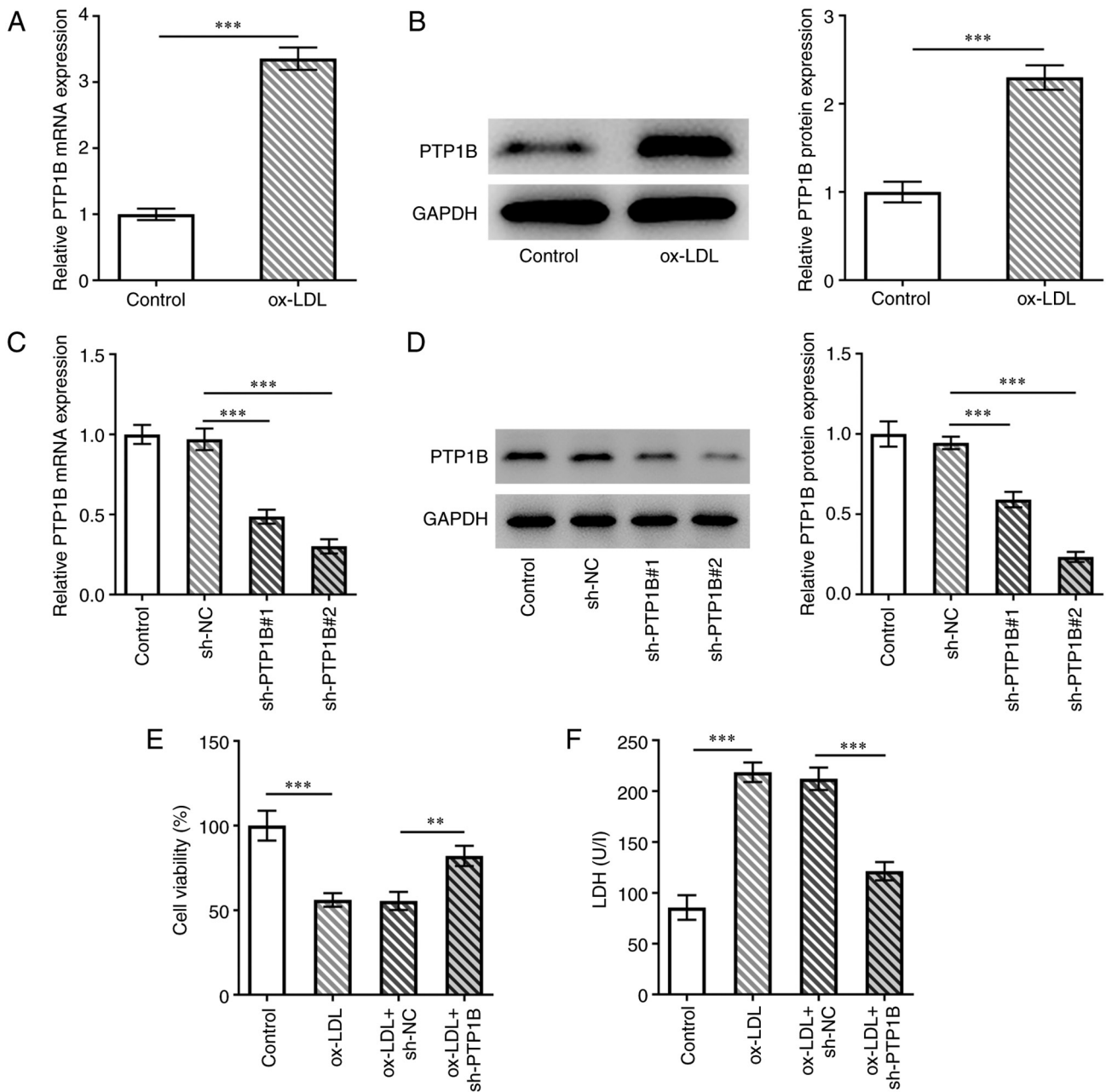
Figure 1. Knockdown of PTP1B expression restores the viability of ox-LDL-induced HUVECs. (A) mRNA and (B) protein expression level of PTP1B in HUVECs with or without ox-LDL treatment were detected by RT-qPCR and western blotting assays. (C) mRNA and (D) protein expression levels of PTP1B in HUVECs transfected with or without sh-PTP1B were detected by RT-qPCR and western blotting assays. (E) Cell viability was measured using Cell Counting Kit-8 assay. (F) LDH level was analyzed using a corresponding kit. Results represent the mean ± SD. **P<0.01 and ***P<0.001. PTP1B, protein tyrosine phosphatase 1B; ox-LDL, oxidized low-density lipoprotein; RT-qPCR, reverse transcription-quantitative PCR; sh, short-hairpin; LDH, lactate dehydrogenase; NC, negative control.

the expression of PTP1B in HUVECs was measured. PTP1B mRNA and protein expression levels were significantly increased in ox-LDL-induced cells compared with those in the control group (Fig. 1A and B). Subsequently, sh-PTP1B constructs were transfected into HUVECs to knock down PTP1B expression. The results from the RT-qPCR and western blotting experiments demonstrated that the PTP1B mRNA and protein expression levels were significantly reduced following transfection with sh-PTP1B#1 or shPTP1B#2 (Fig. 1C and D). Since sh-PTP1B#2 demonstrated a greater transfection efficiency, it was selected for subsequent experiments (Fig. 1C and D). Cell viability was then assessed using

the CCK-8 assay. The results demonstrated that ox-LDL significantly reduced the cell viability of HUVECs, which was in turn reversed by PTP1B silencing (Fig. 1E). Furthermore, significantly increased LDH activity was observed in ox-LDL-treated cells compared with the control group, which was also reversed by sh-PTP1B transfection in response to ox-LDL (Fig. 1F).

PTP1B knockdown alleviates ox-LDL-induced inflammatory damage in HUVECs. To evaluate the effects of PTP1B silencing on inflammatory injury in HUVECs in response to ox-LDL, parameters of inflammation and cell apoptosis were measured.
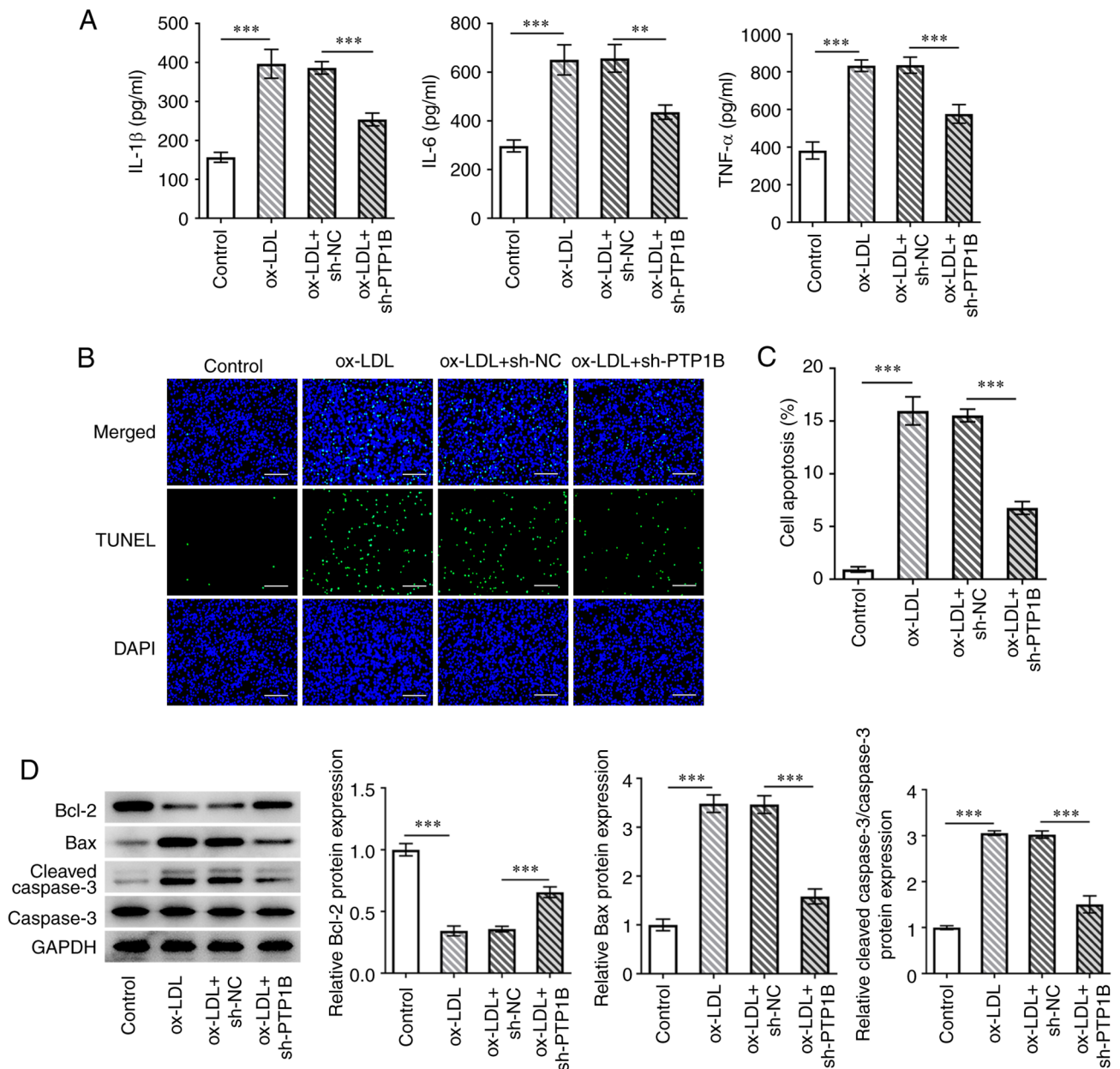
Figure 2. PTP1B knockdown inhibits ox-LDL-induced inflammatory injury of HUVECs. (A) The levels of IL-6, IL-1β and TNF-α were detected using ELISA. (B) Cell apoptosis was measured by TUNEL assay. Scale bar, 50 μm. (C) Histogram of the quantified apoptosis rate of HUVECs. (D) Protein expression levels of Bcl-2, Bax, cleaved caspase-3 and caspase-3 were measured and semi-quantified via western blotting. Results represent the mean ± SD. **P<0.01 and ***P<0.001. PTP1B, protein tyrosine phosphatase 1B; ox-LDL, oxidized low-density lipoprotein; sh, short-hairpin; NC, negative control.

The results demonstrated that ox-LDL treatment significantly enhanced IL-6, IL-1β and TNF-α levels compared with those in the control group (Fig. 2A). However, sh-PTP1B transfection counteracted these effects of ox-LDL on the three inflammatory factors aforementioned (Fig. 2A). Furthermore, cell apoptosis was found to be significantly increased by ox-LDL, which was reversed following the knockdown of PTP1B expression (Fig. 2B and C). Western blotting results demonstrated a significant reduction in the Bcl-2 protein expression levels and a significant increase in Bax and cleaved caspase-3 protein expression levels in ox-LDL-treated cells compared with those in the control group (Fig. 2D). However, the effects of ox-LDL on the expression of these aforementioned proteins associated with apoptosis were reversed by PTP1B knockdown (Fig. 2D).

PTP1B knockdown suppresses ox-LDL-induced oxidative stress in HUVECs and restores tubule-formation ability. Subsequently, the role of PTP1B in oxidative stress in HUVECs induced by ox-LDL was explored. The results demonstrated that ox-LDL treatment significantly increased MDA levels whilst significantly decreasing SOD and GSH-Px activity compared with those in the control group (Fig. 3A). By contrast, PTP1B knockdown significantly reversed the increase in MDA levels whilst also reversing the reduction in SOD and GSH-Px activity following ox-LDL treatment (Fig. 3A). The effects of PTP1B on the tubule-formation ability of HUVECs were investigated. Ox-LDL significantly reduced the number of tubules compared with that in the control group, which was also significantly reversed by PTP1B
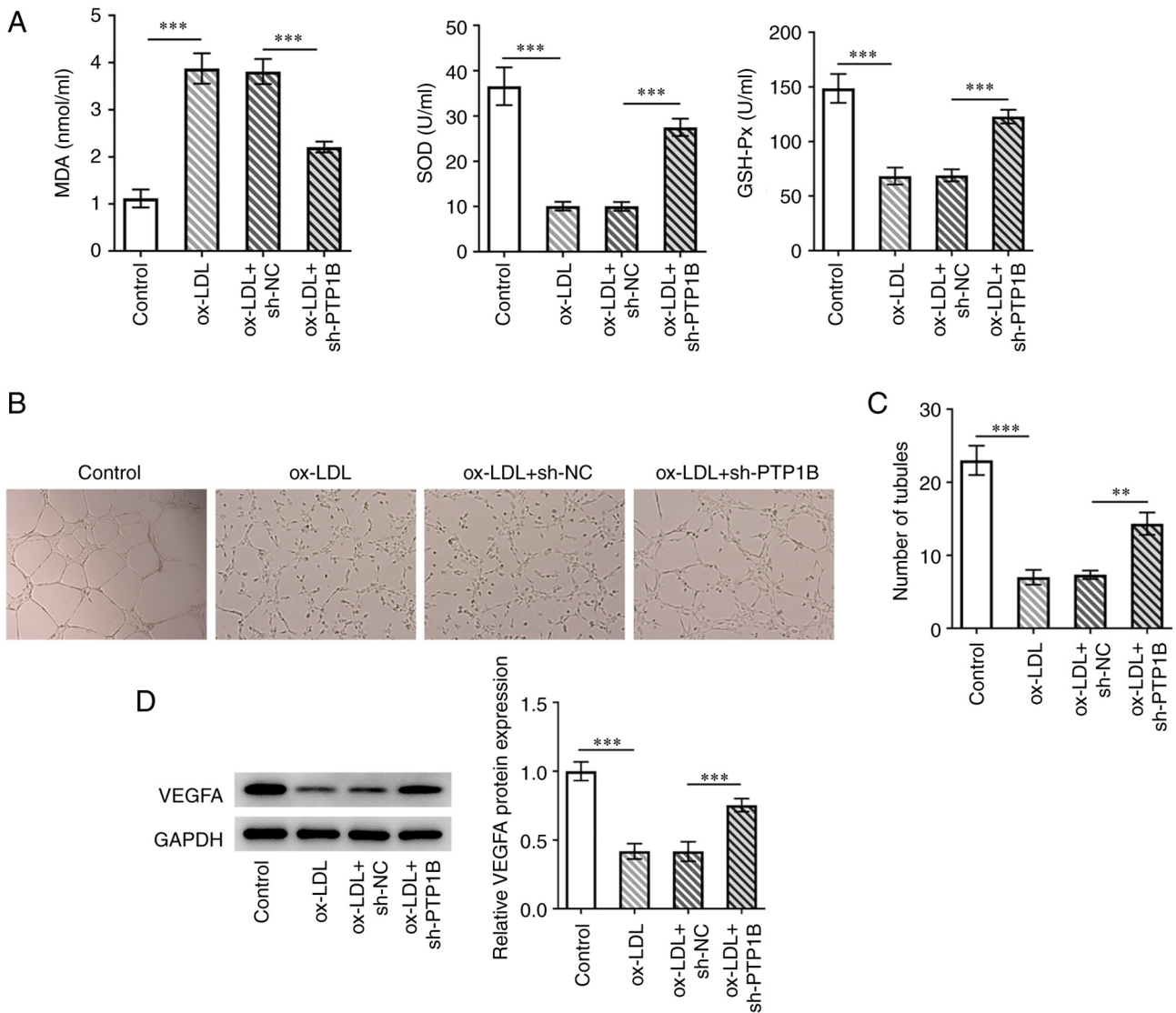
Figure 3. Knockdown of PTP1B expression alleviates ox-LDL-induced oxidative stress in HUVECs to restore tubule-formation ability. (A) Levels of MDA, SOD and GSH-Px were evaluated using corresponding kits. (B) Tubule-formation ability was explored using endothelial tubule formation assay and (C) quantified. Magnification, x40. (D) VEGFA protein expression was measured using western blotting. Results represent the mean ± SD. **P<0.01 and ***P<0.001. MDA, malondialdehyde; SOD, superoxide dismutase; GSH-Px, glutathione peroxidase; PTP1B, protein tyrosine phosphatase 1B; ox-LDL, oxidized low-density lipoprotein; sh, short-hairpin; VEGFA, vascular endothelial growth factor A; NC, negative control.

knockdown (Fig. 3C and D). Furthermore, western blotting demonstrated that ox-LDL significantly reduced VEGFA expression in HUVECs compared with that in control cells, while a significant increase in VEGFA protein expression was observed in ox-LDL-treated HUVECs following PTP1B knockdown compared with that in cells treated with ox-LDL alone (Fig. 3D).

KLF2 negatively regulates PTP1B transcription. Using the JASPAR database, the transcription factor KLF2, was predicted to bind to the PTP1B promoter (Fig. 4A). KLF2 mRNA and protein expression levels were both found to be significantly reduced in HUVECs following treatment with ox-LDL (Fig. 4B and C). To explore the effects of KLF2 on PTP1B in HUVECs, KLF2 was overexpressed and transfection efficiency was verified, as evidenced by the significantly increased KLF2 expression in cells transfected with the Ov-KLF2 plasmid compared with that in cells transfected with the Ov-NC plasmid

(Fig. 4D and E). It was demonstrated that the luciferase activity of the wild-type PTP1B promoter was significantly inhibited by KLF2 overexpression, whereas the mutant PTP1B promoter group displayed no changes in the luciferase activity (Fig. 4F). ChIP was performed to further verify the potential binding of KLF2 on the PTP1B promoter. The results demonstrated that the PTP1B DNA sequence was significantly enriched in the KLF2 group compared with that in the IgG group (Fig. 4G). Furthermore, KLF2 overexpression significantly inhibited the expression of both PTP1B mRNA and protein compared with that in cells transfected with the Ov-NC plasmid (Fig. 4H and I). This suggested a negative regulatory mechanism exerted by KLF2 against PTP1B expression in HUVECs.

KLF2 knockdown reverses the protective effects of PTP1B silencing on ox-LDL-induced HUVECs by regulating the AMPK/SIRT1 signaling pathway. To investigate the role of KLF2 in ox-LDL-treated HUVECs with PTP1B expression
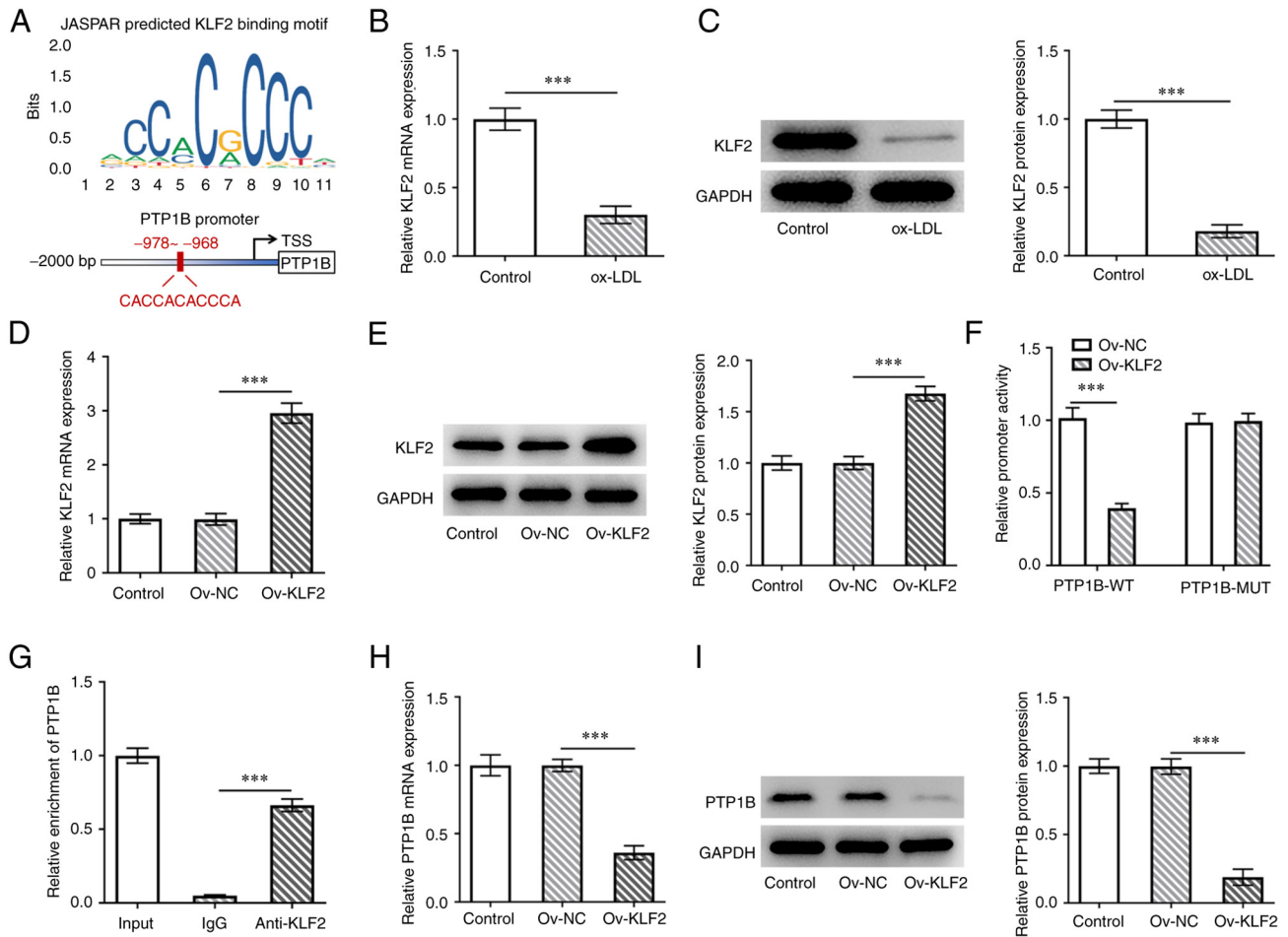
Figure 4. PTP1B transcription is negatively regulated by KLF2. (A) A binding site of KLF2 on the PTP1B promoter was predicted using the JASPAR database. (B) mRNA and (C) protein expression of KLF2 in HUVECs with or without ox-LDL treatment were measured via RT-qPCR and western blotting. (D) mRNA and (E) protein expression of KLF2 in HUVECs transfected with or without Ov-KLF2 were detected using RT-qPCR and western blotting. (F) Dual-luciferase reporter assay was used to verify the binding of KLF2 on the PTP1B promoter. (G) The binding ability of KLF2 on the PTP1B promoter was detected using chromatin immunoprecipitation assay. (H) mRNA and (I) protein expression of PTP1B in HUVECs transfected with or without Ov-KLF2 were detected via RT-qPCR and western blotting. Results represent the mean ± SD. ***P<0.001. KLF2, Kruppel-like factor 2; PTP1B, protein tyrosine phosphatase 1B; ox-LDL, oxidized low-density lipoprotein; Ov, overexpression plasmid; NC, negative control; WT, wild-type; MUT, mutant; RT-qPCR, reverse transcription-quantitative PCR; TSS, transcription start site.

knocked down, sh-KLF2 was transfected into HUVECs and KLF2 expression was prominently decreased after transfection of sh-KLF2#1/2 plasmids, which verified the transfection efficiency using RT-qPCR and western blotting (Fig. 5A and B). Cells transfected with sh-KLF2#2 exhibited lower expression levels of KLF2 compared with those in the sh-KLF2#1 group (Fig. 5A and B). Therefore, sh-KLF2#2 was used for subsequent experiments. Compared with those in the sh-PTP1B-only group, co-transfection with sh-PTP1B and sh-KLF2 slightly reduced cell viability whilst significantly increasing LDH activity (Fig. 5C and D), indicating a reversal of the protective effects initially exerted by PTP1B knockdown. In addition, IL-6, IL-1β and TNF-α levels in ox-LDL-induced HUVECs were significantly elevated by the knockdown of KLF2 and PTP1B compared with those in cells with only PTP1B expression knocked down (Fig. 5E). KLF2 knockdown also significantly reversed the protective effects mediated by sh-PTP1B transfection against cell apoptosis (Fig. 5F), in addition to the expression levels of Bcl-2, Bax and cleaved caspase-3 (Fig. 6B). Furthermore, KLF2 knockdown

significantly increased MDA levels whilst significantly decreasing SOD and GSH-Px activity compared with those in cells transfected with sh-PTP1B only (Fig. 5G).

The number of tubules formed and VEGFA expression were also significantly reduced in the sh-KLF2 + sh-PTP1B compared with those in the sh-PTP1B-only group (Fig. 6A and B). The results of the western blotting assay demonstrated that ox-LDL significantly reduced the levels of AMPK phosphorylation and SIRT1 expression (Fig. 6C). However, sh-PTP1B transfection significantly reversed these effects of ox-LDL on the AMPK/SIRT1 signaling pathway (Fig. 6C). Furthermore, subsequent knockdown of both KLF2 and PTP1B significantly counteracted these regulatory effects of sh-PTP1B on AMPK phosphorylation and SIRT1 expression (Fig. 6C).

Discussion

In the present study, the role of PTP1B in ox-LDL-induced HUVECs was investigated. The results demonstrated that
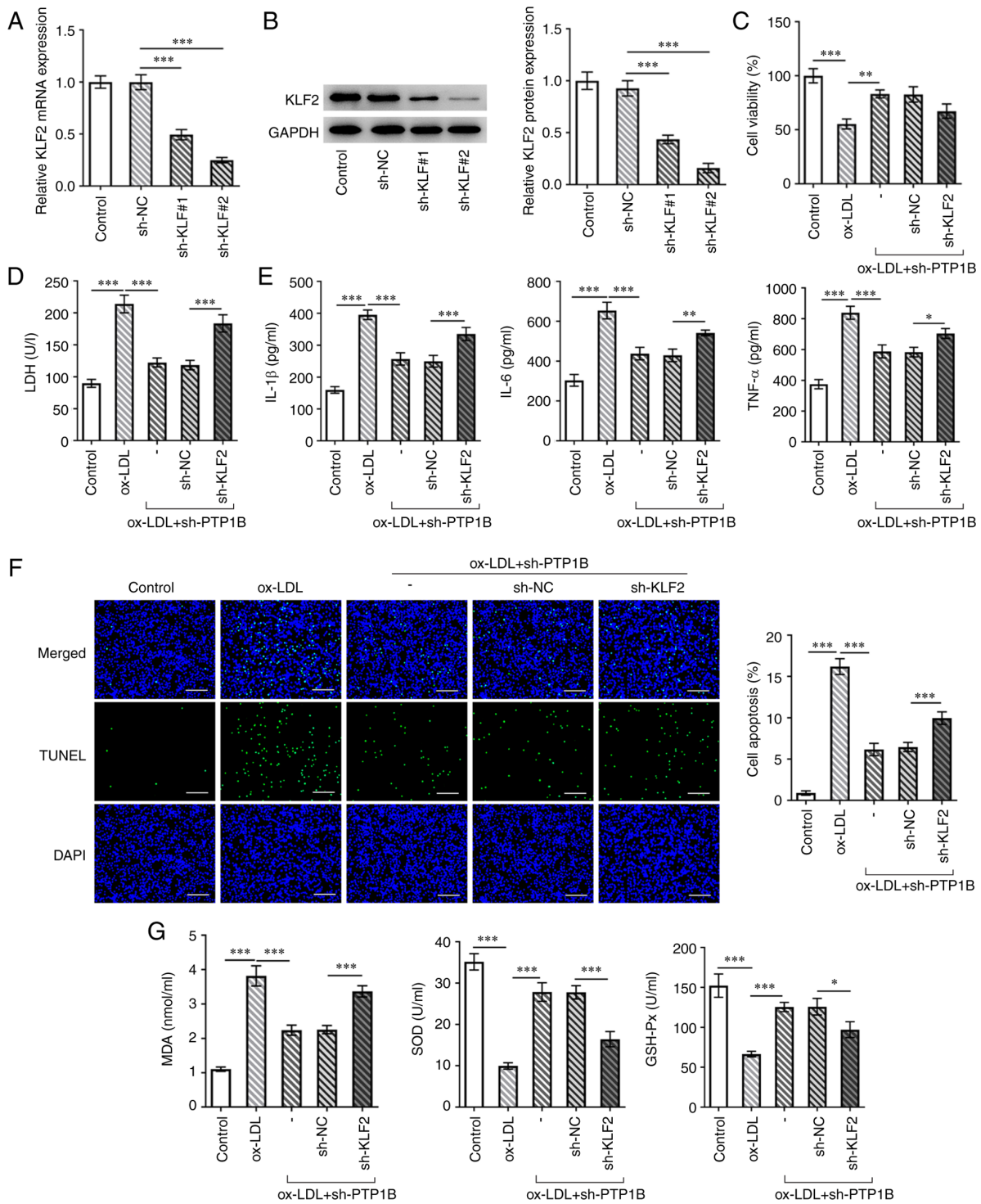
Figure 5. Knocking down KLF2 expression reverses the effect of PTP1B silencing on cell viability, inflammation, apoptosis and oxidative stress in ox-LDL-induced HUVECs. (A) mRNA and (B) protein expression of KLF2 in HUVECs transfected with or without sh-KLF2 were measured using reverse transcription-quantitative PCR and western blotting. (C) Cell viability was measured using Cell Counting Kit-8 assay. (D) LDH levels were analyzed using a corresponding kit. (E) The levels of IL-6, IL-1β and TNF-α were measured using ELISA. (F) Cell apoptosis was measured using TUNEL assay. Scale bar, 50 µm. (G) Levels of MDA, SOD and GSH-Px were assessed using corresponding kits. Results represent the mean ± SD. *P<0.05, **P<0.01 and ***P<0.001. KLF2, Kruppel-like factor 2; PTP1B, protein tyrosine phosphatase 1B; ox-LDL, oxidized low-density lipoprotein; Ov, overexpression plasmid; NC, negative control; sh, short hairpin; LDH, lactate dehydrogenase; MDA, malondialdehyde; SOD, superoxide dismutase; GSH-Px, glutathione peroxidase.

PTP1B knockdown significantly restored cell viability, inhibited inflammatory cell injury whilst also restoring tubule formation ability. Furthermore, the results demonstrated that PTP1B expression was negatively regulated by KLF2, which may be associated with the AMPK/SIRT1 signaling pathway.

Atherosclerosis is a chronic inflammatory disease that is caused by abnormal responses of the blood vessel wall to a number of noxious stimuli (28-30). Vascular EC injury is considered to be a common pathological cause of cardiovascular diseases (31). HUVECs have been widely acknowledged to be
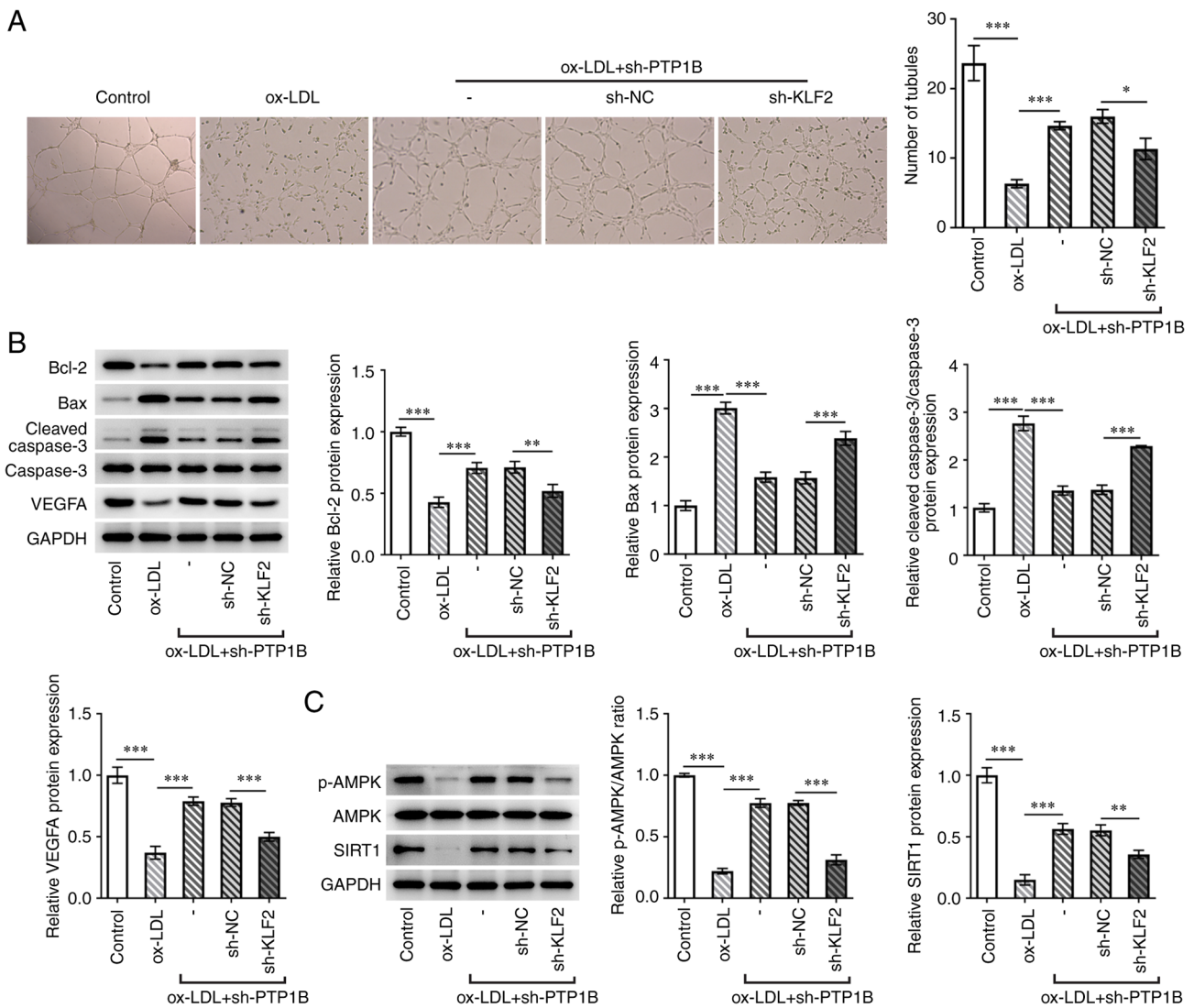
Figure 6. Silencing of KLF2 expression reverses the protective effects of PTP1B knockdown on ox-LDL-induced HUVECs by regulating the AMPK/SIRT1 pathway. (A) Tubule-formation capacity was measured by endothelial tube formation assay. Magnification, x40. (B) Protein expression levels of Bcl-2, Bax, cleaved caspase-3, caspase-3 and VEGFA were measured using western blotting assay. (C) Protein levels of p-AMPK, AMPK and SIRT1 were measured using western blotting. Results represent the mean ± SD. *P<0.05, **P<0.01 and ***P<0.001. KLF2, Kruppel-like factor 2; PTP1B, protein tyrosine phosphatase 1B; ox-LDL, oxidized low-density lipoprotein; NC, negative control; sh, short hairpin; VEGFA, vascular endothelial growth factor A; p-, phosphorylated; AMPK, 5'AMP-activated protein kinase; SIRT1, sirtuin 1.

a useful model for research on the human vascular endothelium (32-35). Although this model does not represent all EC types in an organism, it is nevertheless a viable model for studying the main molecular pathways and properties underlying endothelial functions (36). Ox-LDL can accelerate EC inflammation, apoptosis and endothelial-mesenchymal transition, which serves a key role in mediating the early stages of lesion formation during atherosclerosis (37). Ox-LDL also triggers lipid metabolism disorders, leading to EC injury and death (38). In the present study, ox-LDL stimulation was used to establish an *in vitro* atherosclerosis model, where a dose of ox-LDL (100 μg/ml) was selected based on previous studies (23-25). The results demonstrated that HUVECs treated with ox-LDL exhibited reduced cell viability, increased inflammatory factor levels, elevated apoptosis rates and reduced tubule formation capabilities, all of which are consistent with previous reports (23,24). PTP1B has been previously reported to serve a role in atherosclerosis and contribute to the pathophysiology of ECs (19,39). The present

study demonstrated that PTP1B expression was upregulated in HUVECs after treatment with ox-LDL. Following PTP1B knockdown, HUVEC viability and tubule formation ability were significantly restored, whereas LDH activity, inflammatory factor levels and cell apoptosis were suppressed in cells stimulated with ox-LDL. Furthermore, the oxidative stress levels of the cells were also decreased following PTP1B knockdown. These findings were in consistency with previous reports, which showed that the upregulation of the combination of the cAMP response element-binding protein and lysine methyltransferase 5A inhibited the hyperglycemia-induced inflammatory factor levels by regulating PTP1B expression in vascular endothelial cells (40). These results suggested that PTP1B knockdown may protect HUVECs against inflammatory injury and dysfunction induced by ox-LDL.

Transcription factors can regulate the expression levels of target genes by repressing or activating transcription (41,42). Using the JASPAR database, the present study predicted a

binding site of KLF2 on the PTP1B promoter. The results demonstrated that KLF2 mRNA and protein expression levels were decreased in ox-LDL-treated cells compared with those in the control cells. To verify the binding between KLF2 and the PTP1B promoter, dual-luciferase reporter and ChIP assays were performed. The results demonstrated an interaction between KLF2 and the PTP1B promoter. KLFs belong to the zinc finger family of transcription factors that serve key roles in biological processes, including cell proliferation, inflammation and differentiation (43). KLF2 has been previously demonstrated to serve a role in the regulation of inflammatory activation in endothelial cells (44). A previous study reported that IFN regulatory factor 2-binding protein 2 can protect against ox-LDL-induced endothelial inflammation and epithelial-mesenchymal transition by activating KLF2 expression (45). In addition, Li *et al* (46) reported that synoviolin 1 overexpression inhibited the ox-LDL-induced apoptosis of endothelial cells, which was positively regulated by KLF2. Another previous study demonstrated that ox-LDL could reduce the levels of downstream regulators, such as myocyte enhancer factor 2C, where ERK5 ameliorated ox-LDL-induced EC death, inflammation and dysfunction by inhibiting the ERK5/myocyte enhancer factor 2C/KLF2 signaling pathway in an ox-LDL-induced primary human umbilical vein endothelial cell model (47). In agreement with these previous studies, the present study showed that KLF2 knockdown reversed the effects of PTP1B silencing on ox-LDL-induced HUVECs by inhibiting cell viability and endothelial function, whilst promoting inflammation, oxidative stress and apoptosis.

In conclusion, the present study demonstrated that PTP1B may serve a regulatory role in inflammation and endothelial dysfunction in ox-LDL-induced HUVECs. The results also suggested that PTP1B expression is negatively regulated by KLF2, which may be dependent on the AMPK/SIRT1 signaling pathway. The present study provided a potential novel therapeutic target for the treatment of endothelial dysfunction that occurs during atherosclerosis.

Availability of data and materials

The datasets used and/or analyzed during the current study are available from the corresponding author on reasonable request.

Authors' contributions

YZ and QG designed the study. YZ, QG and ZW performed the experiments. YZ and ZW analyzed the data. All authors read and approved the final manuscript. YZ and OG confirm the authenticity of all the raw data.

Ethics approval and consent to participate

Not applicable.

Patient consent for publication

Not applicable.

Competing interests

The authors declare that they have no competing interests.

References

1. Davies PF, Zilberberg J and Helmke BP: Spatial microstimuli in endothelial mechanosignaling. Circ Res 92: 359-370, 2003.
2. Feaver RE, Gelfand BD and Blackman BR: Human haemodynamic frequency harmonics regulate the inflammatory phenotype of vascular endothelial cells. Nat Commun 4: 1525, 2013.
3. Giannotta M, Trani M and Dejana E: VE-cadherin and endothelial adherens junctions: Active guardians of vascular integrity. Dev Cell 26: 441-454, 2013.
4. Gimbrone MA: The Gordon Wilson lecture. Understanding vascular endothelium: A pilgrim's progress. Endothelial dysfunction, biomechanical forces and the pathobiology of atherosclerosis. Trans Am Clin Climatol Assoc 121: 115-127, 2010.
5. Garcia-Cardeña G, Comander J, Anderson KR, Blackman BR and Gimbrone MA Jr: Biomechanical activation of vascular endothelium as a determinant of its functional phenotype. Proc Natl Acad Sci USA 98: 4478-4485, 2001.
6. Ni CW, Qiu H, Rezvan A, Kwon K, Nam D, Son DJ, Visvader JE and Jo H: Discovery of novel mechanosensitive genes in vivo using mouse carotid artery endothelium exposed to disturbed flow. Blood 116: e66-e73, 2010.
7. Marchio P, Guerra-Ojeda S, Vila JM, Aldasoro M, Victor VM and Mauricio MD: Targeting Early atherosclerosis: A focus on oxidative stress and inflammation. Oxid Med Cell Longev 2019: 8563845, 2019.
8. Tarbell JM, Shi ZD, Dunn J and Jo H: Fluid mechanics, arterial disease, and gene expression. Annu Rev Fluid Mech 46: 591-614, 2014.
9. Chatterjee S and Fisher AB: Mechanotransduction in the endothelium: Role of membrane proteins and reactive oxygen species in sensing, transduction, and transmission of the signal with altered blood flow. Antioxid Redox Signal 20: 899-913, 2014.
10. Chiu JJ and Chien S: Effects of disturbed flow on vascular endothelium: Pathophysiological basis and clinical perspectives. Physiol Rev 91: 327-387, 2011.
11. Su G, Sun G, Liu H, Shu L, Zhang J, Guo L, Huang C and Xu J: Niacin suppresses progression of atherosclerosis by inhibiting vascular inflammation and apoptosis of vascular smooth muscle cells. Med Sci Monit 21: 4081-4089, 2015.
12. Onat D, Brillon D, Colombo PC and Schmidt AM: Human vascular endothelial cells: A model system for studying vascular inflammation in diabetes and atherosclerosis. Curr Diab Rep 11: 193-202, 2011.
13. Chen PY, Qin L, Baeyens N, Li G, Afolabi T, Budatha M, Tellides G, Schwartz MA and Simons M: Endothelial-to-mesenchymal transition drives atherosclerosis progression. J Clin Invest 125: 4514-4528, 2015.
14. Yip SC, Saha S and Chernoff J: PTP1B: A double agent in metabolism and oncogenesis. Trends Biochem Sci 35: 442-449, 2010.
15. Penafuerte C, Feldhammer M, Mills JR, Vinette V, Pike KA, Hall A, Migon E, Karsenty G, Pelletier J, Zogopoulos G and Tremblay ML: Downregulation of PTP1B and TC-PTP phosphatases potentiate dendritic cell-based immunotherapy through IL-12/IFNγ signaling. Oncoimmunology 6: e1321185, 2017.
16. Xu Q, Wu N, Li X, Guo C, Li C, Jiang B, Wang H and Shi D: Inhibition of PTP1B blocks pancreatic cancer progression by targeting the PKM2/AMPK/mTOC1 pathway. Cell Death Dis 10: 874, 2019.
17. da Silva JF, Alves JV, Bolsonni JA, Costa RM, Rios FJ, Camargo LL, Montezano AC, Touyz RM and Tostes RC: Protein tyrosine phosphatase type 1B (PTP1B) contributes to atherosclerotic processes by mechanisms that involve NADPH-oxidase and calcium influx. FASEB J 34: 1-1, 2020.

18. Thompson D, Morrice N, Grant L, Le Sommer S, Lees EK, Mody N, Wilson HM and Delibegovic M: Pharmacological inhibition of protein tyrosine phosphatase 1B protects against atherosclerotic plaque formation in the LDLR$^{-/-}$ mouse model of atherosclerosis. Clin Sci (Lond) 131: 2489-2501, 2017.
19. Thompson D, Morrice N, Grant L, Le Sommer S, Ziegler K, Whitfield P, Mody N, Wilson HM and Delibegović M: Myeloid protein tyrosine phosphatase 1B (PTP1B) deficiency protects against atherosclerotic plaque formation in the ApoE$^{-/-}$ mouse model of atherosclerosis with alterations in IL10/AMPKα pathway. Mol Metab 6: 845-853, 2017.
20. Maupoint J, Besnier M, Gomez E, Bouhzam N, Henry JP, Boyer O, Nicol L, Mulder P, Martinet J and Richard V: Selective vascular endothelial protection reduces cardiac dysfunction in chronic heart failure. Circ Heart Fail 9: e002895, 2016.
21. Ali MI, Ketsawatsomkron P, Belin de Chantemele EJ, Mintz JD, Muta K, Salet C, Black SM, Tremblay ML, Fulton DJ, Marrero MB and Stepp DW: Deletion of protein tyrosine phosphatase 1b improves peripheral insulin resistance and vascular function in obese, leptin-resistant mice via reduced oxidant tone. Circ Res 105: 1013-1022, 2009.
22. Herren DJ, Norman JB, Anderson R, Tremblay ML, Huby AC and Belin de Chantemèle EJ: Deletion of protein tyrosine phosphatase 1B (PTP1B) enhances endothelial cyclooxygenase 2 expression and protects mice from type 1 diabetes-induced endothelial dysfunction. PLoS One 10: e0126866, 2015.
23. Zhou H, Jiang F and Leng Y: Propofol ameliorates ox-LDL-induced endothelial damage through enhancing autophagy via PI3K/Akt/m-TOR pathway: A novel therapeutic strategy in atherosclerosis. Front Mol Biosci 8: 695336, 2021.
24. Zhang Z, Pan X, Yang S, Ma A, Wang K, Wang Y, Li T and Liu S: miR-155 promotes ox-LDL-induced autophagy in human umbilical vein endothelial cells. Mediators Inflamm 2017: 9174801, 2017.
25. Shiotsugu S, Okinaga T, Habu M, Yoshiga D, Yoshioka I, Nishihara T and Ariyoshi W: The biological effects of interleukin-17A on adhesion molecules expression and foam cell formation in atherosclerotic lesions. J Interferon Cytokine Res 39: 694-702, 2019.
26. Livak KJ and Schmittgen TD: Analysis of relative gene expression data using real-time quantitative PCR and the 2(-Delta Delta C(T)) method. Methods 25: 402-408, 2001.
27. Wang XH, Shu J, Jiang CM, Zhuang LL, Yang WX, Zhang HW, Wang LL, Li L, Chen XQ, Jin R and Zhou GP: Mechanisms and roles by which IRF-3 mediates the regulation of ORMDL3 transcription in respiratory syncytial virus infection. Int J Biochem Cell Biol 87: 8-17, 2017.
28. Fava C and Montagnana M: Atherosclerosis is an inflammatory disease which lacks a common anti-inflammatory therapy: How human genetics can help to this issue. A narrative review. Front Pharmacol 9: 55, 2018.
29. Galkina E and Ley K: Immune and inflammatory mechanisms of atherosclerosis (*). Annu Rev Immunol 27: 165-197, 2009.
30. Tousoulis D, Oikonomou E, Economou EK, Crea F and Kaski JC: Inflammatory cytokines in atherosclerosis: Current therapeutic approaches. Eur Heart J 37: 1723-1732, 2016.
31. Sun HJ, Hou B, Wang X, Zhu XX, Li KX and Qiu LY: Endothelial dysfunction and cardiometabolic diseases: Role of long non-coding RNAs. Life Sci 167: 6-11, 2016.
32. Pan JX: LncRNA H19 promotes atherosclerosis by regulating MAPK and NF-kB signaling pathway. Eur Rev Med Pharmacol Sci 21: 322-328, 2017.
33. Watanabe T and Sato K: Roles of the kisspeptin/GPR54 system in pathomechanisms of atherosclerosis. Nutr Metab Cardiovasc Dis 30: 889-895, 2020.
34. Zhu Z, Li J and Zhang X: Salidroside protects against ox-LDL-induced endothelial injury by enhancing autophagy mediated by SIRT1-FoxO1 pathway. BMC Complement Altern Med 19: 111, 2019.
35. Gao W, Liu H, Yuan J, Wu C, Huang D, Ma Y, Zhu J, Ma L, Guo J, Shi H, et al: Exosomes derived from mature dendritic cells increase endothelial inflammation and atherosclerosis via membrane TNF-α mediated NF-κB pathway. J Cell Mol Med 20: 2318-2327, 2016.
36. Baudin B, Bruneel A, Bosselut N and Vaubourdolle M: A protocol for isolation and culture of human umbilical vein endothelial cells. Nat Protoc 2: 481-485, 2007.
37. Yang H, Mohamed AS and Zhou SH: Oxidized low density lipoprotein, stem cells, and atherosclerosis. Lipids Health Dis 11: 85, 2012.
38. Hurtado-Roca Y, Bueno H, Fernandez-Ortiz A, Ordovas JM, Ibañez B, Fuster V, Rodriguez-Artalejo F and Laclaustra M: Oxidized LDL is associated with metabolic syndrome traits independently of central obesity and insulin resistance. Diabetes 66: 474-482, 2017.
39. Legeay S, Fautrat P, Norman JB, Antonova G, Kennard S, Bruder-Nascimento T, Patel VS, Faure S and Belin de Chantemèle EJ: Selective deficiency in endothelial PTP1B protects from diabetes and endoplasmic reticulum stress-associated endothelial dysfunction via preventing endothelial cell apoptosis. Biomed Pharmacother 127: 110200, 2020.
40. Huang T, Li X, Wang F, Lu L, Hou W, Zhu M and Miao C: The CREB/KMT5A complex regulates PTP1B to modulate high glucose-induced endothelial inflammatory factor levels in diabetic nephropathy. Cell Death Dis 12: 333, 2021.
41. Garcia-Alonso L, Iorio F, Matchan A, Fonseca N, Jaaks P, Peat G, Pignatelli M, Falcone F, Benes CH, Dunham I, et al: Transcription factor activities enhance markers of drug sensitivity in cancer. Cancer Res 78: 769-780, 2018.
42. Bushweller JH: Targeting transcription factors in cancer-from undruggable to reality. Nat Rev Cancer 19: 611-624, 2019.
43. Jha P and Das H: KLF2 in regulation of NF-κB-mediated immune cell function and inflammation. Int J Mol Sci 18: 2383, 2017.
44. Zhou Z, Tang AT, Wong WY, Bamezai S, Goddard LM, Shenkar R, Zhou S, Yang J, Wright AC, Foley M, et al: Cerebral cavernous malformations arise from endothelial gain of MEKK3-KLF2/4 signalling. Nature 532: 122-126, 2016.
45. Jiang Y and Shen Q: IRF2BP2 prevents ox-LDL-induced inflammation and EMT in endothelial cells via regulation of KLF2. Exp Ther Med 21: 481, 2021.
46. Li Q, Xuan W, Jia Z, Li H, Li M, Liang X and Su D: HRD1 prevents atherosclerosis-mediated endothelial cell apoptosis by promoting LOX-1 degradation. Cell Cycle 19: 1466-1477, 2020.
47. Patel R, Varghese JF, Singh RP and Yadav UCS: Induction of endothelial dysfunction by oxidized low-density lipoproteins via downregulation of Erk-5/Mef2c/KLF2 signaling: Amelioration by fisetin. Biochimie 163: 152-162, 2019.